AIAA 2001–0441

ERROR CONTROL AND MESH ADAPTATION FOR THE EULER EQUATIONS

X. D. Zhang D. Pelletier J.-Y. Trépanier
R. Camarero

Département de génie mécanique
École Polytechnique de Montréal
Montréal, Québec, Canada, H3C 3A7
and
Centre de Recherche en Calcul Appliqué (CERCA)
Montréal, Québec, Canada, H3X 2H9

39th AIAA Aerospace Sciences Meeting & Exhibit
8-11 January 2001 / Reno, NV

AIAA-2001-0441

ERROR CONTROL AND MESH ADAPTATION FOR THE EULER EQUATIONS

X. D. Zhang* D. Pelletier† J.-Y. Trépanier‡ R. Camarero §

Département de génie mécanique
École Polytechnique de Montréal
Montréal, Québec, Canada, H3C 3A7
and
Centre de Recherche en Calcul Appliqué (CERCA)
Montréal, Québec, Canada, H3X 2H9

Abstract

In this paper, we investigate the efficiency of mesh adaptation process to control the error in the solution of one-dimensional Euler equations. Two strategies are compared to drive the adaptation process: error minimization and error equidistribution. Single error indicators (error in density or residual in continuity equation) and multiple error indicators (error in all variables and/or residual in all equations) are used and compared to guide the mesh adaptation. Numerical tests show that the single indicator of residual in continuity equation and its equidistribution leads to the most efficient way to reduce the global and local errors as well as residual for both subsonic and transonic cases. Multi-error indicator using all the error information is also a good choice but requires more computations for error estimation.

Introduction

The use of adaptive meshes is one of the most attractive strategies to obtain highly accurate solutions in computational fluid dynamics (CFD). The generation of such adapted meshes is usually guided by a proper error estimator or indicator. The ultimate goal of mesh adaptation is to control the discretization error. To achieve this goal, reliable *a posteriori* error estimation is a basic requirement. For elliptic equations and finite element methods, there are many theoretical and practical approaches for reliable *a posteriori* error estimations. For hyperbolic equations, such as the Euler equations of aerodynamics, very few investigations have been conducted.

One of the difficulties for hyperbolic problems is that the solution error is not a local product of the numerical discretization. The locally generated error will be transported somewhere else in the domain because of the propagating nature of the hyperbolic equations. This makes error estimation and control much more complicated. There are many observations about error transport. One well-known behavior is the degradation of accuracy behind a supersonic shock.[1–3] Other discussions can be found in refs.[4,5] Some theoretical analyses about error estimation and control have been provided by Süli and co-workers.[6,7] From these analyses, it is clear that the error which is created somewhere may be propagated elsewhere. What controls the transported error should be the information at locations where the errors are created not at locations where the errors have accumulated. For linear problems, the linear equation for the solution error is totally controlled by the residual of the discretized equations.[4] Thus, the estimation of the error indicator for guiding grid adaptation must include information from the residual of the equations, not simply the solution error. When error transport is dominant, the residual based error indicator is more reliable than the solution error as has been shown in ref.[8] using only the residual in continuity equation and exact error in momentum. The importance and advantages of using residual based error indicator for error control via mesh adaptation has been analyzed and verified through a single variable. This paper investigates the same approach but using error in all variables and/or residual in all equations. Generally, errors in different variables lead to different optimal meshes because of their difference in error location as well as in error magnitude. How we can obtain a mesh

*Research Professional, Member AIAA
†Professor, Associate Fellow AIAA
‡Associate Professor, Member AIAA
§Professor, Member AIAA

which is optimal to minimize and control all those errors is not an obvious task. Some issues concerning multiple error information will be addressed.

The goal of this work is to develop rigorous mesh adaptive strategies for the Euler equations. The objective is to assess error estimators based on evaluation of residual and solution error; and to assess two adaptive strategies driving the error estimators: h-remeshing and node relocation; and to study the feasibility of combining estimators for all variables and/or for all equations in one robust adaptation strategy.

Error Estimation and Control

Global control of the solution error is generally termed *a priori* error estimate for a specific numerical method. It ensures convergence of the method when the mesh size tends to zero. Global error control may be expressed as

$$||u - u_h||_{W,\Omega} = \mathcal{O}(h^\alpha), \text{ with } h = \max_{K \in \mathcal{P}_h}(h_K) \quad (1)$$

where $||\cdot||_{W,\Omega}$ is a proper norm over the whole domain of interest Ω in a Sobolev space W, $\mathcal{P}_h$ is the mesh of a partition established over $\bar{\Omega}$, h_K represents the size (length) of the element (cell) $K \in \mathcal{P}_h$. The superscript $\alpha > 0$ is the rate of convergence. For elliptic equations and finite element method, this error estimate with $W = H^1(\Omega)$ can be found in reference.[9] For hyperbolic equations and finite volume method, similar results with L_2 norm were given in reference.[10]

This type of error estimate guarantees that the true error of the solution is controlled globally by refining the mesh **everywhere**. However, most mesh adaptive strategies rely on local control of the error, i.e.

$$||u - u_h||_{W,K} = \mathcal{O}(h_K^\alpha), \quad \text{for } K \in \mathcal{P}_h. \quad (2)$$

If this condition can be established, then local mesh refinement based on the solution error can control the local error, and consequently control the global error as well. However, to the author's knowledge, very little theoretical work has been done concerning such type of local error estimation. Most applications have simply assumed that it is true[11,12] for elliptic equations. However, this is questionable for hyperbolic equations. If it does not hold for some equations, then any adaptive strategy utilizing the error information to locally refine the mesh will lead to inefficient control of the error. This point of view has been demonstrated in ref.[4] and will be readdressed in this paper.

The exact error is not always available for most problems of interest. To be able to control the true error globally, one relies on a specific error estimator and try to control the estimated error instead. However, the purpose of using adaptive technique to control the estimated error is to ultimately allow us to control the true error. This requires that the estimated error must have a behavior similar to the true one. The efficiency index defined by

$$\theta = \frac{||e||}{||u - u_h||}$$

for an estimated error $||e||$ is a measure for its reliability and efficiency.

Advantage of using residual error indicator

A brief review about residual-based error estimation and control can be found in ref.[8] for both elliptic and hyperbolic equations. From the discussions, residual type error estimators have long been known and used effectively for both elliptic and hyperbolic equations. For elliptic equations, residual based estimators and solution error based estimators are essentially equivalent. Differences concern only their robustness and simplicity. For hyperbolic equations, residual based estimators often assumes that the cell error ε^{cell} dominates the transported error ε^{trans},[13,14] i.e.

$$||\varepsilon_K^{trans}|| \ll ||\varepsilon_K^{cell}||, \quad \text{for every } K \in \mathcal{P}_h.$$

As demonstrated in refs.,[4,5] this is a strong restriction for hyperbolic equations. In many cases, the distributions of $||\varepsilon_K^{cell}||$ and $||\varepsilon_K^{trans}||$ can be very different and in some cell K, one has

$$||\varepsilon_K^{trans}|| \gg ||\varepsilon_K^{cell}||.$$

Further more, the distributions of the true error $||\varepsilon_K||$ and residual $||h_K r_K||$ can also be very different.

In a recent effort, Houston & Süli[5] suggested to solve an error equation for cases when the transported error is dominant. This equation provides an error estimator for the true error. The authors have also conducted such a procedure in a similar fashion, and demonstrated that the true error can be estimated very accurately.[4,15,16] However, a more reliable error indicator for mesh adaptation seems to be a residual based one rather than the error based one, even if one knows the exact error (see ref.[4] as well as the following section). The reasons can be attributed to the following facts:

(i) The local residual can be controlled by the local mesh size. Consequently local mesh refinement

based on the residual leads to a decrease of both the local and global residuals. As a result, a global decrease of solution error can be achieved.

(ii) The local true error (thus any error based error estimator) is difficult to control through the local mesh size, since the transported error originates from elsewhere. The source of the transported error is represented by the residual.[4] Consequently local mesh refinement driven by this type of error estimator cannot always control the true error locally and globally, at least not efficiently.

In summary, the use of residual based error indicator for mesh adaptation offers the following advantages (especially for hyperbolic equations):

- Conceptually, residuals are more straightforward to estimate than solution errors;
- It is not clear whether any (global or local) error control is possible when refinement is driven by the local error;
- Refinement based on local residuals results in global and local residual control. Thus global error control is achieved;
- Residual based estimators show comparable or better effectiveness to that of other error estimator for elliptic equations;
- A residual based error indicator is a measure of how accurately the *equations* have been solved. Thus it provides control over the discretization error.

Problem Description

The error indicators are used to adapt the mesh efficiently so as to control the discretization error and improve solution accuracy. To achieve this goal, one requires that at least the error indicators and the true error tend to zero together during the mesh adaptation process. For elliptic equations, one requires the so-called property of asymptotic exactness.[17] However, for hyperbolic equations, very little work can be found about the convergence rate and asymptotic exactness of error estimators and indicators because of the lack of mathematical foundations. As these properties are very important for error control, numerical verifications for some simple practical problems have been conducted using uniform meshes in ref.[18] for a quasi one-dimensional Euler system. In this paper, efforts are concentrated on verification of mesh adaptation using different error indicators.

Consider a steady quasi one-dimensional Euler system representing compressible flow in a duct of variable cross-section

$$u_t + [f(u)]_x = s, \tag{3}$$

in which

$$u = \mathcal{D}\begin{pmatrix} \rho \\ \rho v \\ \rho e \end{pmatrix}, f(u) = \mathcal{D}\begin{pmatrix} \rho v \\ \rho v^2 + p \\ \rho v e + v p \end{pmatrix}, s = \begin{pmatrix} 0 \\ p\frac{\partial \mathcal{D}}{\partial x} \\ 0 \end{pmatrix}.$$

where ρ is the density, v the fluid velocity, e the specific total energy and p the pressure. For the quasi-one-dimensional problem, closed form solutions can be calculated when the area function $\mathcal{D}(x)$ is known.[19]

Only one geometry has been used and the corresponding area function is given by

$$\mathcal{D}(x) = \begin{cases} d_1 & 0.0 \le x \le 0.5 \\ d_1 - k(x-0.5)^2 & 0.5 < x \le 1.5 \\ 2.25 - \frac{2}{3}\text{atan}(4(x-2.5)) & 1.5 < x \le 3.0 \\ a(x-2) + b/(x-2) & 3.0 < x \le 6.0 \\ d_2 + d_3[1-(x-7)^2] & 6.0 < x \le 7.0 \\ d_2 + d_3 & 7.0 < x \le 8.0 \end{cases}$$

where, $k = 4/51$, $a = 1.125 - 4/15 - atan(2)/3$, $b = 1.125 + 4/15 - atan(2)/3$, $d_1 = 2.25 + k - 2atan(-4)/3$, $d_2 = 4a + b/4$ and $d_3 = (a - b/16)/2$ are constants. This function is a piecewise C^∞ smooth and C^1 smooth at the joining points. To reduce the effect of boundary condition treatment, the nozzle is extended at both ends by a length of constant cross-section duct. The geometry of the nozzle is shown in Fig. 1.

First, we consider a shockless subsonic flow. At the inlet, pressure is extrapolated from the first cell value while other variables are computed using isentropic flow condition. At the outflow boundary, the normalized back pressure is set to $p = 0.93$ and the velocity and the temperature are extrapolated from the last cell. The second test is for a transonic nozzle with a shock downstream of the throat. The shock is set at $x = 5.2$ when the back pressure is specified as $p = 0.75$. The inlet pressure is extrapolated from the first cell and other properties are computed from isentropic relations. At the outlet, the velocity and the temperature are extrapolated.

A explicit finite-volume time-marching scheme is used to solve the quasi-1D Euler equations (3). The interface flux are computed using a modified Roe's characteristic upwind flux-difference-splitting scheme to treat the source term more accurately.[20] With those modifications, the scheme is second-order accurate for steady state solutions over smooth flow regions. For details about the scheme and modifications, one is referred to ref. 20.

The solution errors for a system of equations are quite complicated. For the governing equations stated above, there are three independent variables. Different set of variables, such as primitive or conservative, provide different values for solution errors.

Previous work[18] shows that the estimated error using Richardson extrapolation agrees very well with the true error. The convergence rate is almost asymptotically exact except in the vicinity of a shock. This is because the theory, based on Taylor series expansion, is not valid across discontinuities. The approaches based on solution reconstruction and error equations provided very accurate error estimations when applied to a conserved variable. For non-conservative variables, an adjustment due to an error in the flux must be added in order to achieve better agreement.

From verifications on quasi one-dimensional problems,[18] both the L_1 and L_2 norms of the errors yield second-order convergence rates for flows without shock. For flows with shocks, the L_2 norm yields a convergence rate of only one half, while the L_1 norm is of first-order convergence rate which agrees with the accepted statements. For the residual of the continuity equation, both the L_1 and L_2 norms exhibit second-order convergence rate for flows without shock but are 0^{th} and $-1/2$ for flows with shocks. For such cases, a proper error indicator based on residual for grid adaptation must be multiplied by the local grid size h_i to ensure convergence. The resulting rate of convergence of this modified estimator will be the same as for shockless flows. Also, the L_1 norm is less sensitive to smoothness of the geometry. Thus, it seems that the L_1 norm of the error estimators will be more reliable than the L_2 norm for grid adaptation and error control.

The weak norm in H^{-1} was proposed by Süli & Houston[6] for the flow with shocks. However, as demonstrated in ref.,[18] the use of residual in a weak norm to control the true error in H^{-1} norm may not be as efficient as one would expect since the efficiency index approaches infinity. For flows without shock its efficiency index tends to a non unit constant. However, the stronger norms in L_1 and L_2 are much easier to compute and behave in the same way. So, in the present investigation of grid adaptation, only L_1 norms of the residual and exact error in ϕ will be used.

Mesh Adaptation and Error Control

Mesh Adaptation strategies

We study two strategies for grid adaptation. One is to minimize the estimated error in which the mesh will be refined only when the local error indicator is not sufficiently small. Another one is to equidistribute the estimated error by remeshing with fixed total number of cells. Details are described below.

Error minimization

The local error indicator denoted by $||e||_i$ is computed in each cell. Here $||\cdot||$ represents the L_1 norm. The global error is defined by $||e|| = \sum ||e||_i$, and the relative error is defined by $\eta = ||e||/||\phi||$. Generally speaking, one cannot refine the mesh to infinitesimal levels of the error. Instead, we search for a grid with the smallest number of cells which can reduce the relative error η to a specified target value $\bar{\eta}$.

In practice, one refines the mesh only where necessary. Hence, we refine the mesh only when the local ratio ξ_i satisfies

$$\xi_i = \frac{||e||_i}{\bar{e}_m} > 1.$$

where $\bar{e}_m = \bar{\eta}(||\phi|| + ||e||)/m$ and m the number of cells involved.

If we assume $||e||_i \propto h_i^p$, where h_i is the current mesh size and p the rate of convergence, then, to satisfy the requirement

$$\xi_i \leq 1. \tag{4}$$

the target mesh size is given by[12]

$$h_{target} = h_i \xi_i^{-1/p}. \tag{5}$$

By requiring this, the total number of cells is approximately $M \approx Int(\int_0^8 \frac{1}{h_{target}} dx)$. If one wants to prespecify the total number of cells N, rescaling of the target mesh size h_{target} by M/N is needed.

Error equidistribution

In order to achieve equidistribution of the error indicator, one can fix the total number of cells N and repeat the adaptive process by node relocation until a stopping criterion is satisfied. By doing this, the error cannot be arbitrarily reduced. It will tend to a minimum constant. However, the stopping criterion is not a trivial condition to specify for this strategy. Ideally, if the error indicator is equidistributed over the whole domain, the error ratio of its mean and maximum values will be one and the grid points will stop moving (the grid has converged to its ultimate one). However, in practice, this is almost impossible. Instead, one may require that the ratio be greater than a specified value. Numerical tests show that the above mentioned stopping criteria is not always easy to reach, especially for the residual error indicator.

Some results using single error indicator (error in density, residual in continuity equation) have been

presented in ref.[8] It was shown that the two strategies lead to different grid spacing and error distributions. Generally speaking, the minimization technique is easier to implement and more rapid to reach the stopping requirement. However, it is not very efficient to equidistribute the error. On the other hand, the equidistribution strategy often control better the averaging error indicator but has difficulty to satisfy a stopping criterion. Moreover, it is not clear how the equidistribution in the case of multi-error indicators can be handled. In the present work, detailed investigations on the performance of these two mesh adaptation strategies in controlling multi-error information are presented.

Combination of multiple errors

When many variables and many equations must be taken into account, the errors from every variables and residual from each equations should be used to guide the mesh adaptation. There are, of course, many ways of combining all this error information. Ideally, we could solve different variable or equation over differently optimized meshes. However, difficulties in implementation and errors from interpolation of variables between these meshes will be encountered.

In this paper, we rely on using a single error indicator to guide a single mesh adaptation but we try to include many error sources. The local error indicator is defined by

$$e_{ind} = ||\bar{e}|| \max_{1\le j\le k}(\frac{e_j}{||e_j||})$$

where k is the number of errors, e_j may represents the solution error in variables or the residual error in equations, $||e_j||$ the global norm of error e_j and $||\bar{e}||$ is the averaged global error

$$||\bar{e}|| = \frac{1}{k}\sum_j ||e_j||.$$

In the following discussions, especially in the figures, "*rsd_all*" means all the residual errors in the three equations of continuity (mass), momentum and energy (k=3), "*err_all*" means all the solution errors in all three conservative variables $(\rho, \rho u, \rho e)$ (k=3), "*rsd_err_all*" represents all errors from variables and equations (k=6). To distinguish from the multi-error indicator, "*rsd_mass*" used to denote the residual error in the mass equation (k=1) and "*err_density*" for the error in density (k=1).

The way to estimate the errors in each variable can be very different. To measure the efficiency of using error as an error indicator and to prevent extra errors from error estimation, in this paper, we use the true errors in all variables directly, as the closed form solution exits for the quasi-one-dimensional Euler equations. To evaluate the residual error estimate in equation discretization, we use two methods to compute them. First, since the equations are discretized by upwinding scheme which is basically first-order accurate, a direct differentiation using central difference over the flux components is used to represent the truncation errors in equation discretization. Second, the source term in the error equation approach is a good measure of the residual error in equation discretization,[4] which is computed based on the Taylor expansion in the modified equations. The former one is noted as "*rsd_mass*" and the latter is represented by "*src_mass*".

Numerical examples

A subsonic case

The strategy of error minimization is verified first. The starting mesh is always uniform with 40 cells. Once the value of $\bar{\eta}$ is specified, a remeshing procedure is applied based on the error indicators and is repeated until the criteria (4) is satisfied. This procedure usually requires 5 to 10 iterations to reach convergence. However, when grid spacing becomes very small (for large number of points M), sometimes it needs more than 50 iterations to reach the criteria. But the total number of points M and errors were only very slightly modified after 10 iterations. For such cases, we stop the procedure once $\xi \le 2$ and there was no increase in M.

The L_1 and L_2 norms of the error in density (*err_density*) and residual in mass equation (*rsd_mass*) have been used as error indicators to guide the mesh adaptation. The error and residual control based on these two error indicators are plotted in Figs. 2 to 5 and are compared with that obtained using a uniform grid spacing. All figures show that the grid adaptation guided by the residual indicator (*rsd_mass*) exhibits a better performance in controlling the solution error as well as the residual than that using the error indicator (*err_density*). For this case, the L_1 and L_2 norms perform very similarly. The order of convergence of the solutions adapted using residual is almost the same as that of the uniform grids, but the error absolute levels are almost one order of magnitude lower. The grid adaptation based on solution error (*err_density*) fails to control the residual but is able to control the solution error itself with some success. The global errors in L_1 and L_2 norms using both residual evaluation methods (*rsd_mass* vs *src_mass*) have been controlled equally well as shown in Figs. 6 and 7. It is noted that, although using the residual indicator

shows a significant success to control the residual itself compared to using the solution error when M is small, it becomes less and less efficient when M increases.

The second strategy consists in fixing the total number of nodes and trying to equidistribute the error indicators. As mentioned before, the criteria used to stop the adaptive process is not an obvious issue. After 5 to 10 iterations, the global errors changes slightly, but still has some degree of oscillation because of the balance of equidistribution of the local error. To illustrate the global tendency of error control, we repeat the adaptation process for 30 cycles. Then we use an averaged value of its values in the last 10 iterations to demonstrate their global convergence rate in error control.

By choosing different total number of cells N (40, 80, 160, 320 and 640), the performance of the two error indicators in L_1 and L_2 norms has been verified versus the number of cells. The global error and residual are plotted in Figs. 8 and 11 to show their ability to control them. This time, the error indicators in L_1 and L_2 norms behave quite differently. The error indicator in L_2 norm does not show a consistent rate of convergence. The zigzag tendency is probably caused by the difficulties of equidistributing the error indicators. For the error indicator in L_1 norm, the residual based grid adaptation is always more efficient than the error based one in controlling both the solution error and residual. When the grid is relatively coarse, the difference between the two error indicators is not significant. However, as the grid is refined, the difference becomes more and more evident. The rate of convergence of the adapted solutions based on residual (rsd_mass) is almost the same as that for uniform grids, but with an order of magnitude smaller in absolute error and residual values. However, the grid adaptation based on density error ($err\_density$) exhibits a tendency to reduce efficiency and even becomes less efficient than using uniform grids as the number of cells is increased (Fig. 8). The convergence rate is about one order higher than that using residual indicator (rsd_mass). This is an indication that the use of solution error to guide the grid adaptation may work for coarse grid but it might be a poor choice when the grid becomes sufficiently fine. Again, the control in residual using both error indicators is less efficient as M increases. The convergence rate is about one order higher than that of using the uniform mesh. However, the tendency of residual control is almost the same for both error indicators but with a constant difference between these two error indicators (Fig. 9). Different residual evaluations perform almost the same as shown in Figs. 12 and 13 for both error norms of L_1 and L_2.

Figures 14 to 21 show the control tendencies for the density error, residual in mass equation as well as total error in all variables $(\rho, \rho u, \rho e)$ and total residual in all equations using all multi-error indicators: rsd_all, err_all and $rsd_e rr\_all$ for both mesh adaptation strategies. The total error is defined as $||e||_{total} = \sum_j ||e_j||$. They are also compared to those using single error in density ($err\_density$) and residual (rsd_mass). From Figs. 14 to 17 using the minimization strategy, it seems that all the combinations with residual work better than using purely the error or errors in a variable. The best one is the simplest one of using the residual in the mass equation as an error indicator. The strategy using all six error information (rsd_err_all) showed a good balance in controlling all error quantities. As for the equidistribution strategy from Figs. 18 to 21, the two error indicators using density error ($err\_density$) and errors in three variables (err_all) performed closely (not efficient), but the later one showed a tendency to match the second order convergence rate while the former one is of just first order (Fig. 8). The error indicators using residual or residuals performed much better (close to second order). The combination of all errors in variable and equation (rsd_err_all) provided the best error control. Surprisingly, only the all error indicator (err_all) can match the order of the residual control with uniform meshes when M is sufficiently large as shown in Fig. 19.

If we compare the efficiency for both adaptive strategies by plotting the best one from each strategy as shown in Figs. 22 and 23, we observe that the combination indicator of all errors and residuals (rsd_err_all) with the equidistribution adaptive strategy provides a better compromise in controlling both error and residual. The single residual indicator (rsd_mass) with both strategies is also a very good candidate for mesh adaptation, but requires less computations for the error estimation.

A transonic case

As reported in ref.,[18] the convergence rate for the error in density is only first-order in the L_1 norm and 0^{th} order for the residual in continuity equation for transonic flow with a shock. In order to use the residual as an adaptive indicator, we multiply the residual by the local grid size h, which results in a first-order convergence rate in L_1 norm. Also as discussed in ref.,[18] away from the shock, the error and residual are all of second order accuracy in both L_1 and L_2 norms. It is not clear which value of order p ($p = 1$ or $p = 2$) should be used in eq. (5) in order

to have a better error control. The first test is on the use of $p = 1$ or $p = 2$. Fig. 24 and 25 plot the error in density and residual in the mass equation using both values of $p = 1$ and $p = 2$ with error equidistribution strategy. It is observed that $p = 2$ always produces better control in both the error and residual. Thus, in the following test for the transonic flow case, the value of p in eq. (5) is always set as 2.

The error minimization strategy is also verified first. The global error in density and residual in continuity equation with L_1 norm have been plotted in Figs. 26 and 27. The convergence rate for uniform grid spacing is of only first-order. The adapted grid using all these error indicators show much better convergence rate (at least second order). Contrary to the subsonic case, the grid adaptation guided by the error in density ($err\_density$) resulted in a better control of the error and residual than the one guided by the residual in mass equation (rsd_mass), but they have almost the same convergence rate. Mesh adaptations based on both indicators worked reasonably well in the sense that very efficient control of the solution error and equations residual can be achieved with superior convergence. The performance of all other multi-error indicators are somewhat close and almost in between the two single-error indicators. The total error and total residual control in L_1 norm are also plotted in Figs. 28 and 29 in which similar behaviors can be found.

The error equidistribution strategy is also applied to the transonic case with different fixed number of cells N (40, 80, 160 and 320). The error in density and residual in the mass equation with L_1 norm have been plotted in Figs. 30 and 31. Again, higher convergence rates for all the error indicators have been obtained than with uniform meshes. This time, the grid adaptation guided by the residual in the mass equation (rsd_mass) resulted in a better control than the one guided by the error in density ($err\_density$), not only in error magnitudes but also in convergence rate. All other multi-error indicators yield very close results and are in between the two single-error indicators. Fig. 32 demonstrate similar performances for controlling the total error in all variables.

If we compare the efficiency for both adaptive strategies by plotting the best one from each side as shown in Figs. 33 and 34, it is observed that the single residual indicator (rsd_mass) with the equidistribution adaptive strategy provides the best compromise to control both errors and residuals. The combination indicator of all errors and residuals (rsd_err_all) with equidistribution strategy is also a very good candidate for mesh adaptation, but requires more computations for the error estimation.

Concluding remarks

In this work, we have discussed two strategies of mesh adaptation to control the error for the Euler equations, i.e. the error minimization and error equidistribution. Numerical tests with subsonic and transonic flows have been conducted and presented using error indicators estimated from a single- and multi-error of variables or equations. From these results, it seems that the single residual indicator (rsd_mass) and the combination indicator of all errors and residuals (rsd_err_all) with equidistribution strategy yield the most efficient way to reduce the error in the variables and residuals in equations for both subsonic and transonic cases. The single residual indicator (rsd_mass) should be chosen as the first candidate for practical applications as it requires much less computing time for residual estimation. However, for the minimization strategy, its simplicity and fast convergence in mesh adaptation is also an important factor to consider for complicated applications. It is showed again that, for mesh adaptations, the L_1 error norm is easier to handle that the L_2 error norm. When transonic flow with shocks is considered, a more appropriate value for the order of the methods p, in evaluating the target mesh size, is $p = 2$ even though the order of the global convergence is about 1 for the L_1 norm.

In the present work, only a simple one-dimensional case is considered and verified extensively. Similar investigations need to be conducted for two- and three-dimensional problems before it may become useful for more complex practical applications.

Acknowledgments

This work was sponsored in part by NSERC of Canada, FCAR of Québec, Bombardier Aerospace and the Air Force Office of Scientific Research under grant AFOSR F49620-96-1-0329.

References

[1]Casper, J. and Carpenter, M., "Computational considerations for the simulation of shock-induced sound," *SIAM J. Sci. Comput.*, Vol. 19, No. 3, May 1998, pp. 813–828.

[2]Carpenter, M. and Casper, J., "Accuracy of shock capturing in two spatial dimensions," *AIAA Journal*, Vol. 37, No. 9, September 1999, pp. 1072–1079.

[3]Roache, P., *Verification and Validation in Computational Science and Engineering*, Hermosa Publishers, Albuquerque, New Mexico, USA, 1998.

[4]Zhang, X. D., Trépanier, J.-Y., and Camarero, R., "A Posteriori Error Estimation Method for Finite-Volume Solutions of Hyperbolic Conservation Laws," *Comput. Method in Appl. Mech. Eng.*, Vol. 185, No. 1, April 2000, pp. 1–19.

[5]Houston, P. and Süli, E., "A posteriori error indicators for hyperbolic problems," Tech. Rep. 98/14, Oxford Univer-

sity, Computing Laboratory, (also an invited lecture at the ICFD conference, Oxford, April 1998), April 1998.

[6]Süli, E. and Houston, P., "Finite element methods for hyperbolic problems: a posteriori error analysis and adaptivity," Tech. Rep. 96/09, Oxfort Univ., May 1996.

[7]Süli, E., "A posteriori error analysis and adaptivity for finite element approximations of hyperbolic problems," Tech. Rep. 97/21, Oxfort Univ., Comput. Lab., December 1997.

[8]Zhang, X. D., Pelletier, D., Trépanier, J.-Y., and Camarero, R., "Error estimation and control for the Euler equations," *Fluids 2000*, 2000, AIAA Paper 2000-2246, June 19-22, Denver, USA.

[9]Ciarlet, P., *The finite element method for elliptic problems*, North-Holland Publishing Company, Amsterdam, 1978.

[10]Morton, K. and Süli, E., "A posteriori and a priori error analysis of finite volume methods," *The Mathematics of Finite Elements and Applications*, Jone Wiley & Sons Ltd, 1994, Chapter 18, Edited by J.R. Whiteman.

[11]Zienkiewicz, O. and Zhu, J., "A simple error estimator and adaptive procedure for practical engineering analysis," *Int. J. Numer. Meth. Eng.*, Vol. 24, 1987, pp. 337–357.

[12]Zienkiewicz, O. and Taylor, R., *The finite element method, Vol. 1*, McGraw-Hill Book Company, London, 1989.

[13]Mackenzie, J., Sonar, T., and Süli, E., "Adaptive finite volume methods for hyperbolic problems," *The Mathematics of Finite Elements and Applications*, Jone Wiley & Sons Ltd, 1994, Chapter 19, Edited by J.R. Whiteman.

[14]Sonar, T. and Süli, E., "A dual graph-norm refinement indicator for finite volume approximations of the Euler equations," *Numerische Mathematik*, Vol. 78, 1998, pp. 619–658.

[15]Zhang, X. D., Trépanier, J.-Y., and Camarero, R., "An a posteriori error estimation method based on an error equation," *AIAA 15th CFD Conf.*, 1997, pp. 383–397, AIAA Paper 97-1889, June 29-July 2, Snowmass, USA.

[16]Ilinca, C., Zhang, X. D., Trépanier, J.-Y., and Camarero, R., "A comparison of three error estimation techniques for Finite-Volume Solutions of compressible flows," *Comput. Method in Appl. Mech. Eng.*,, Vol. 189, No. 4, October 2000, pp. 1277–1294.

[17]Zhu, J., "A posteriori error estimation — the relationship between different procedures," *Comput. Methods Appl. Mech. Engrg.*, Vol. 150, 1997, pp. 411–422.

[18]Zhang, X. D., Pelletier, D., Trépanier, J.-Y., and Camarero, R., "Verification of error estimators for the Euler equations," AIAA Paper 2000-1001, Reno, USA.

[19]White, F. M., *Fluid Mechanics*, McGraw-Hill, 3rd edition, 1994.

[20]Roe, P., "Characteristic-based schemes for the Euler equations," *Annual review of fluid mechanics*, Vol. 18, 1986, pp. 337–365.

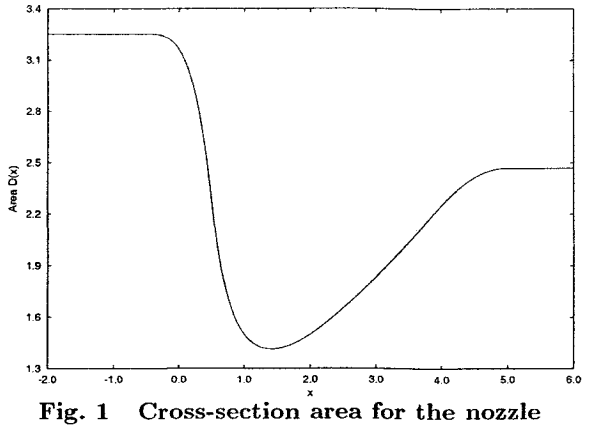

Fig. 1 Cross-section area for the nozzle

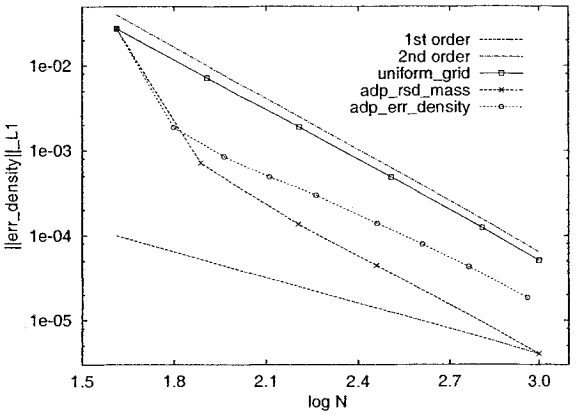

Fig. 2 Error in density in L_1 norm, subsonic case, minimization strategy

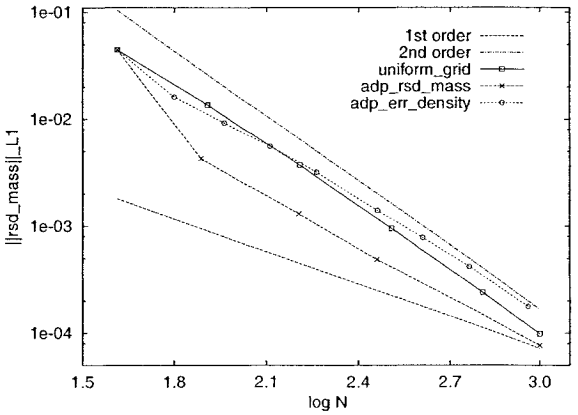

Fig. 3 Residual in mass equation in L_1 norm, subsonic case, minimization strategy

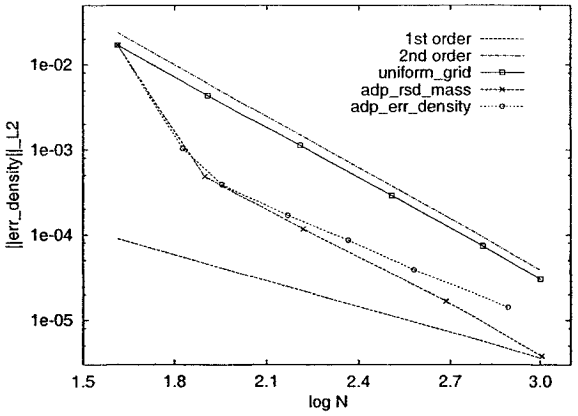

Fig. 4 Error in density in L_2 norm, subsonic case, minimization strategy

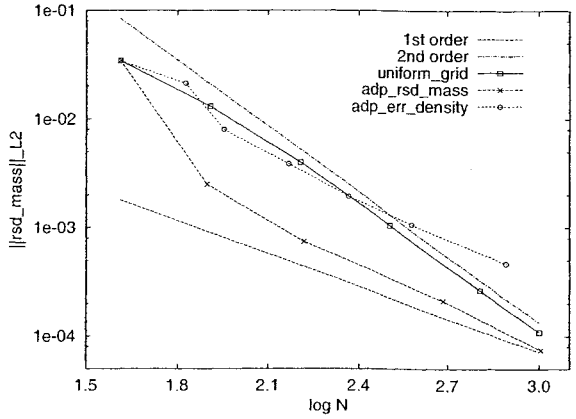

Fig. 5 Residual in mass equation in L_2 norm, subsonic case, minimization strategy

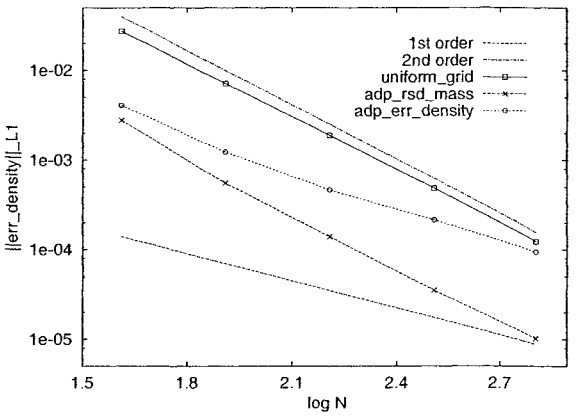

Fig. 8 Error in density in L_1 norm, subsonic case, equidistribution strategy

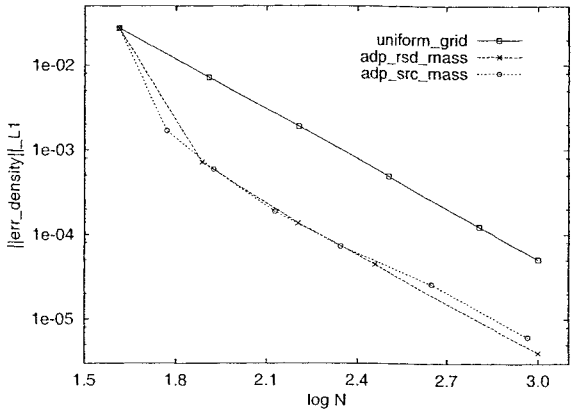

Fig. 6 Error in density in L_1 norm, subsonic case, adapted using different residual evaluation with minimization strategy

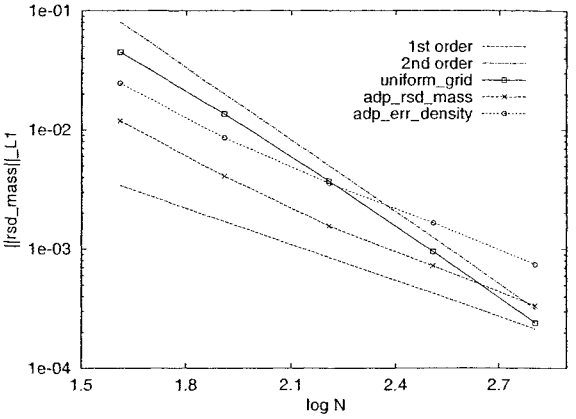

Fig. 9 Residual in mass equation in L_1 norm, subsonic case, equidistribution strategy

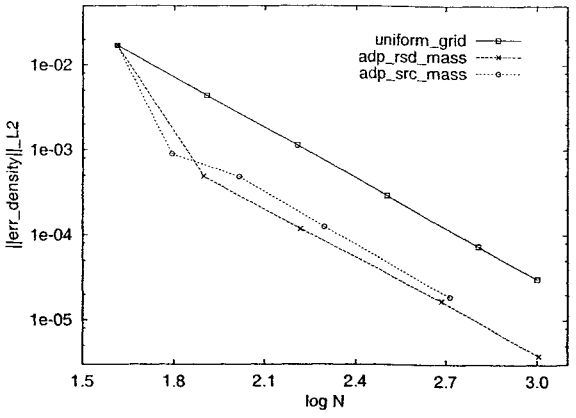

Fig. 7 Error in density in L_2 norm, subsonic case, adapted using different residual evaluation with minimization strategy

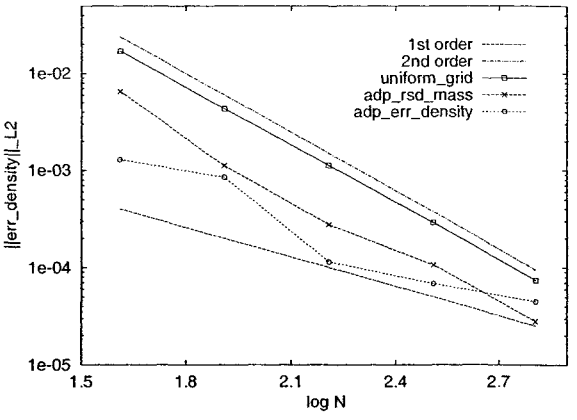

Fig. 10 Error in density in L_2 norm, subsonic case, equidistribution strategy

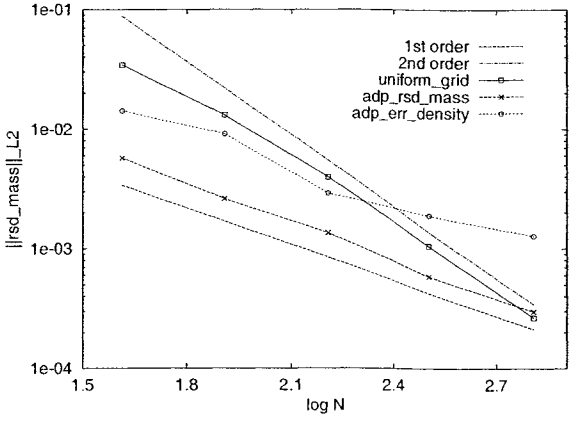

Fig. 11 Residual in mass equation in L_2 norm, subsonic case, equidistribution strategy

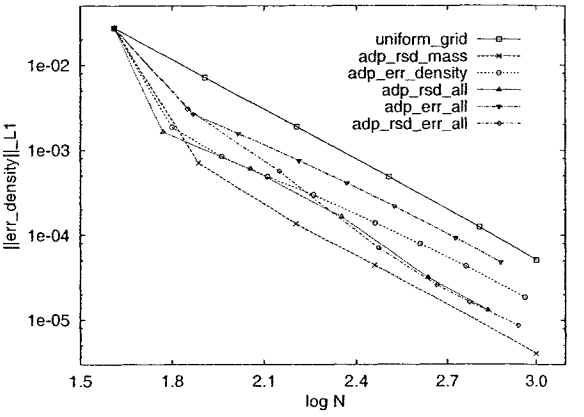

Fig. 14 Error in density, subsonic case, adapted using multi-error indicators with minimization strategy

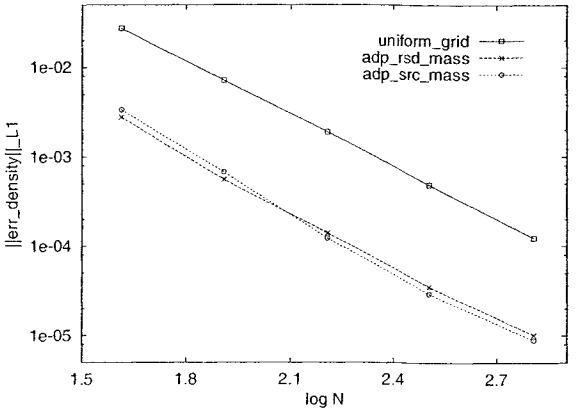

Fig. 12 Error in density in L_1 norm, subsonic case, adapted using different residual evaluation with equidistribution strategy

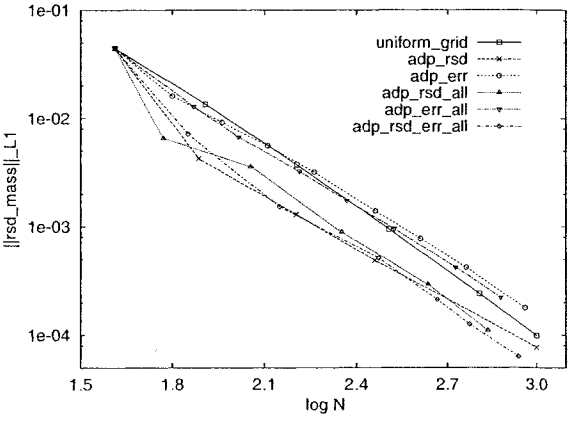

Fig. 15 Residual in mass equation, subsonic case, adapted using multi-error indicators with minimization strategy

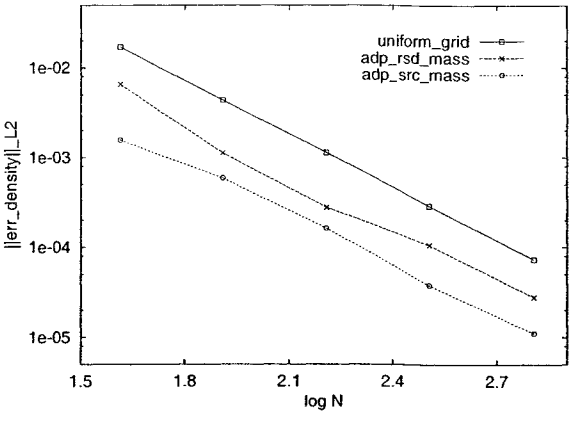

Fig. 13 Error in density in L_2 norm, subsonic case, adapted using different residual evaluation with equidistribution strategy

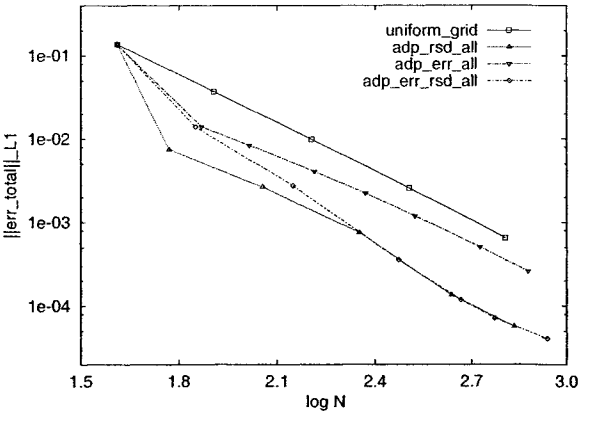

Fig. 16 Total error in all variables, subsonic case, adapted using multi-error indicators with minimization strategy

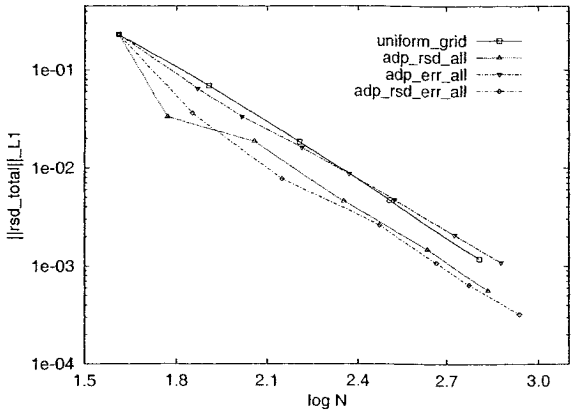

Fig. 17 Total residual in all equations, subsonic case, adapted using multi-error indicators with minimization strategy

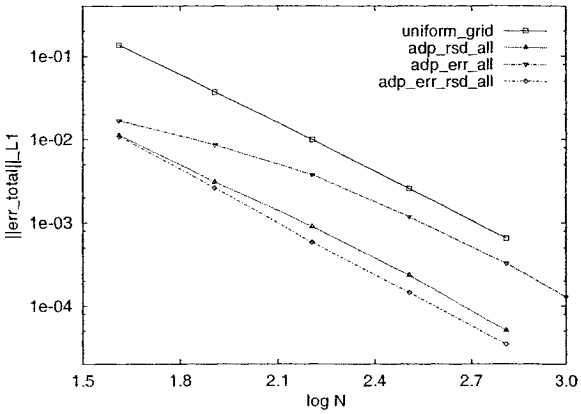

Fig. 20 Total error in all variables, subsonic case, adapted using multi-error indicators with equidistribution strategy

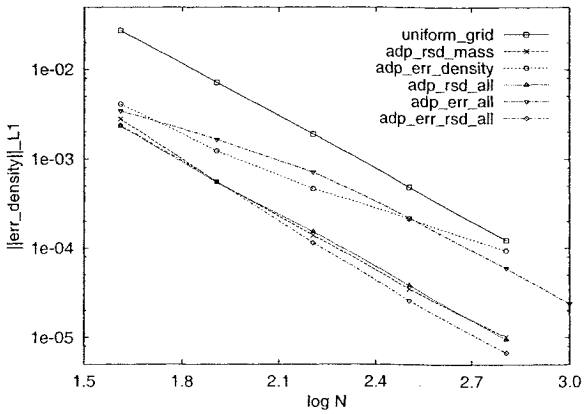

Fig. 18 Error in density, subsonic case, adapted using multi-error indicators with equidistribution strategy

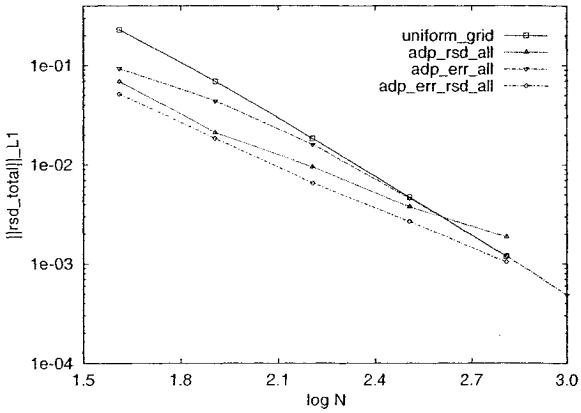

Fig. 21 Total residual in all equations, subsonic case, adapted using multi-error indicators with equidistribution strategy

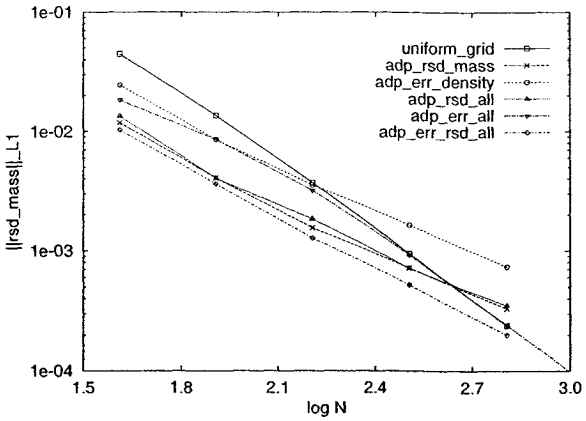

Fig. 19 Residual in mass equation, subsonic case, adapted using multi-error indicators with equidistribution strategy

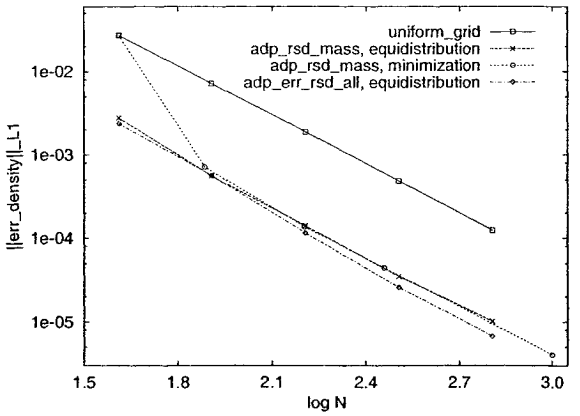

Fig. 22 Comparison of error in density, subsonic case

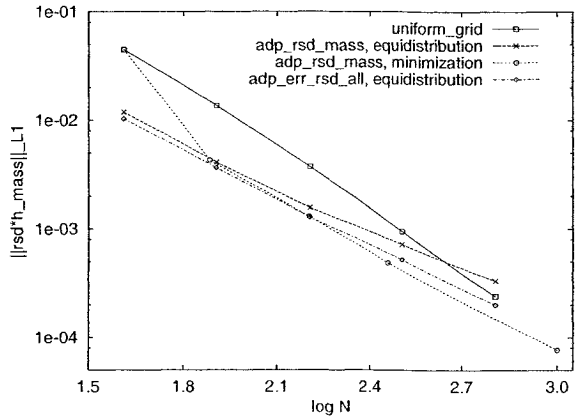

Fig. 23 Comparison of residual in mass equation, subsonic case

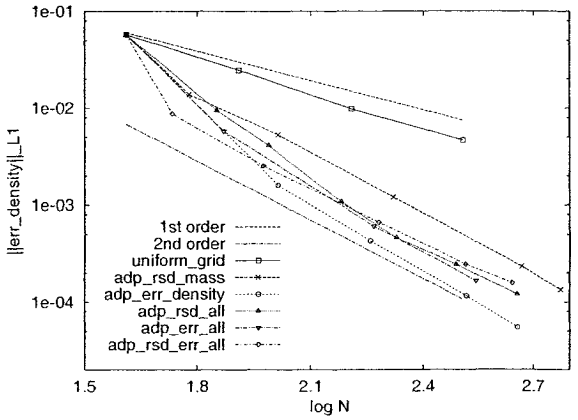

Fig. 26 Error in density, transonic case, minimization strategy

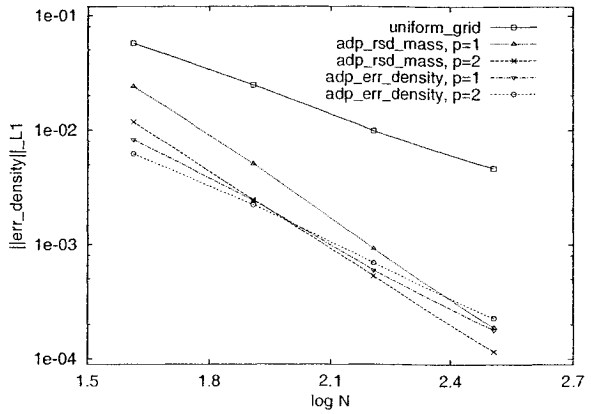

Fig. 24 Error in density comparison for different p, transonic case, equidistribution strategy

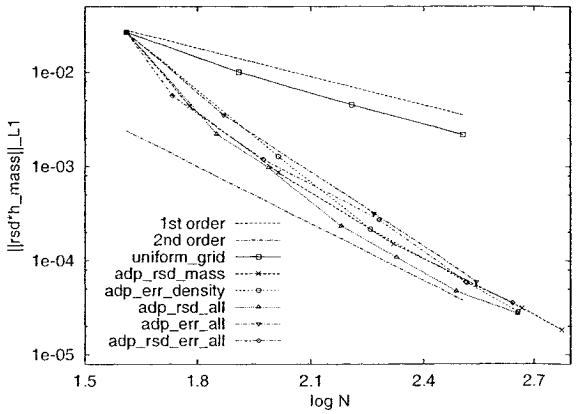

Fig. 27 Residual in mass equation, transonic case, minimization strategy

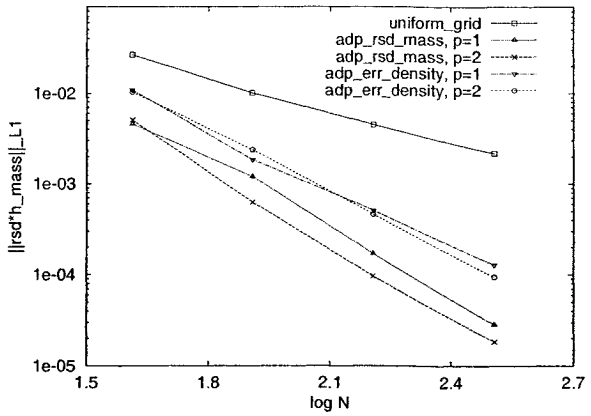

Fig. 25 Residual comparison for different p, transonic case, equidistribution strategy

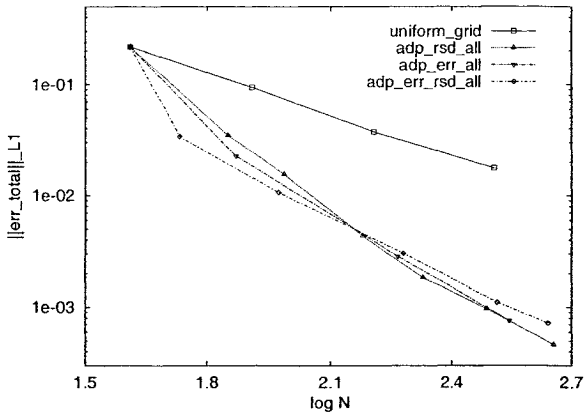

Fig. 28 Total error in all variables, transonic case, minimization strategy

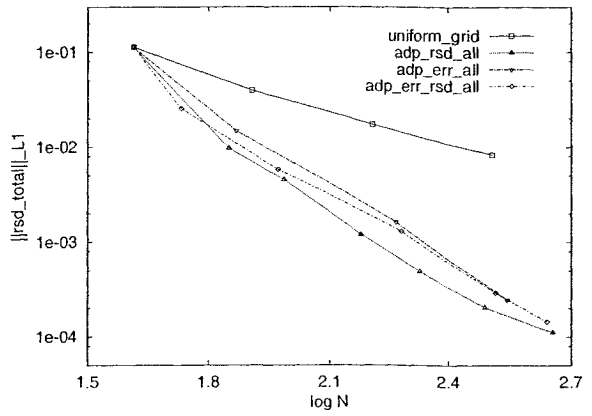

Fig. 29 Total residual in all equations, transonic case, minimization strategy

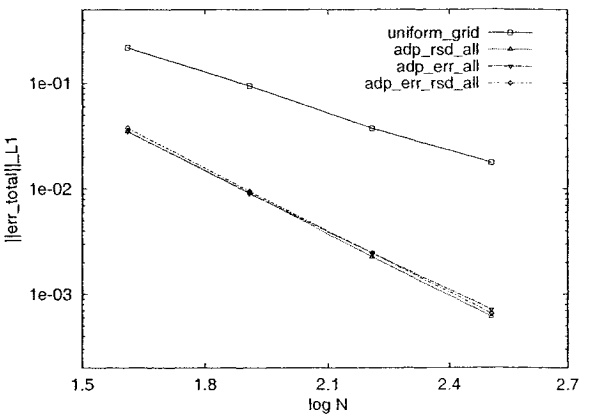

Fig. 32 Total error in all variables, transonic case, equidistribution strategy

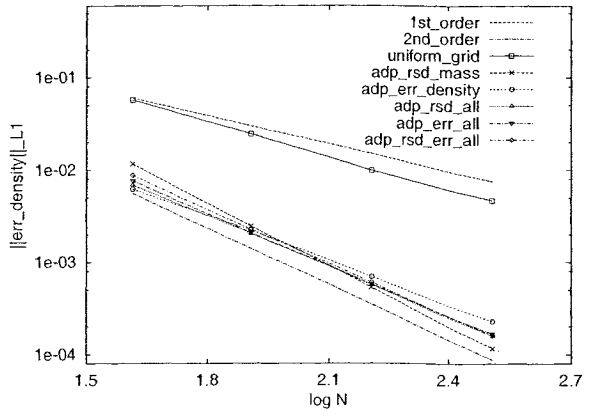

Fig. 30 Error in density, transonic case, equidistribution strategy

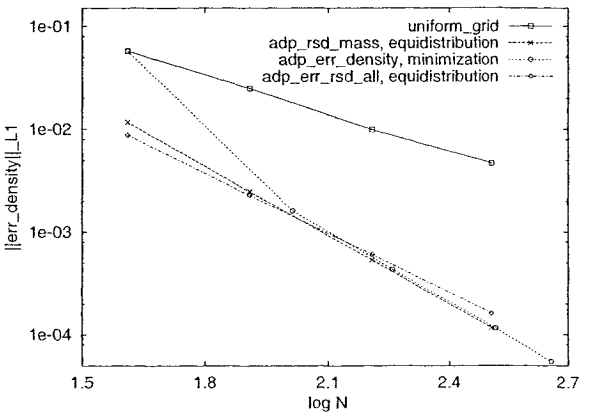

Fig. 33 Comparison of error in density, transonic case

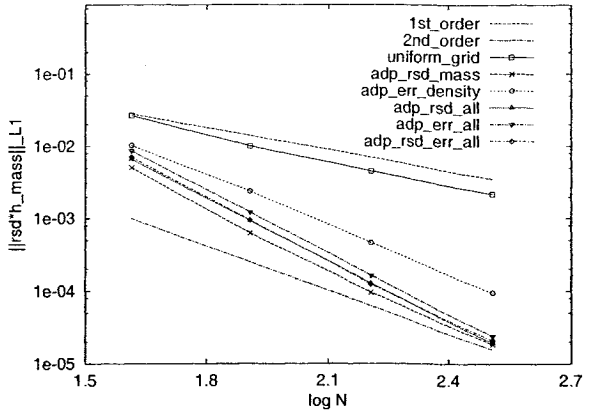

Fig. 31 Residual in mass equation, transonic case, equidistribution strategy

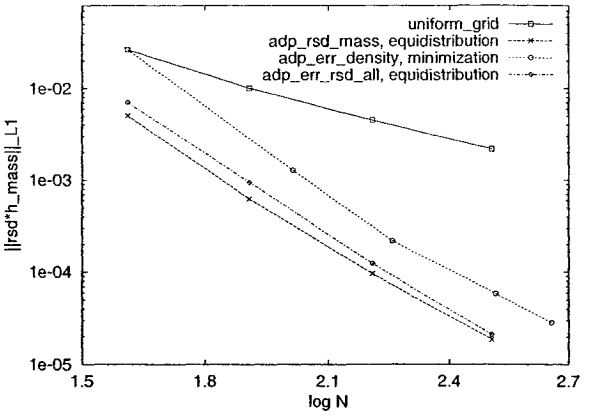

Fig. 34 Comparison of residual in mass equation, transonic case